Cell Reports, Volume *23*

Supplemental Information

Human Pluripotent Stem-Cell-Derived Cortical Neurons Integrate Functionally into the Lesioned Adult Murine Visual Cortex in an Area-Specific Way

Ira Espuny-Camacho, Kimmo A. Michelsen, Daniele Linaro, Angéline Bilheu, Sandra Acosta-Verdugo, Adèle Herpoel, Michele Giugliano, Afsaneh Gaillard, and Pierre Vanderhaeghen

Supplemental Materials

Supplemental Figures

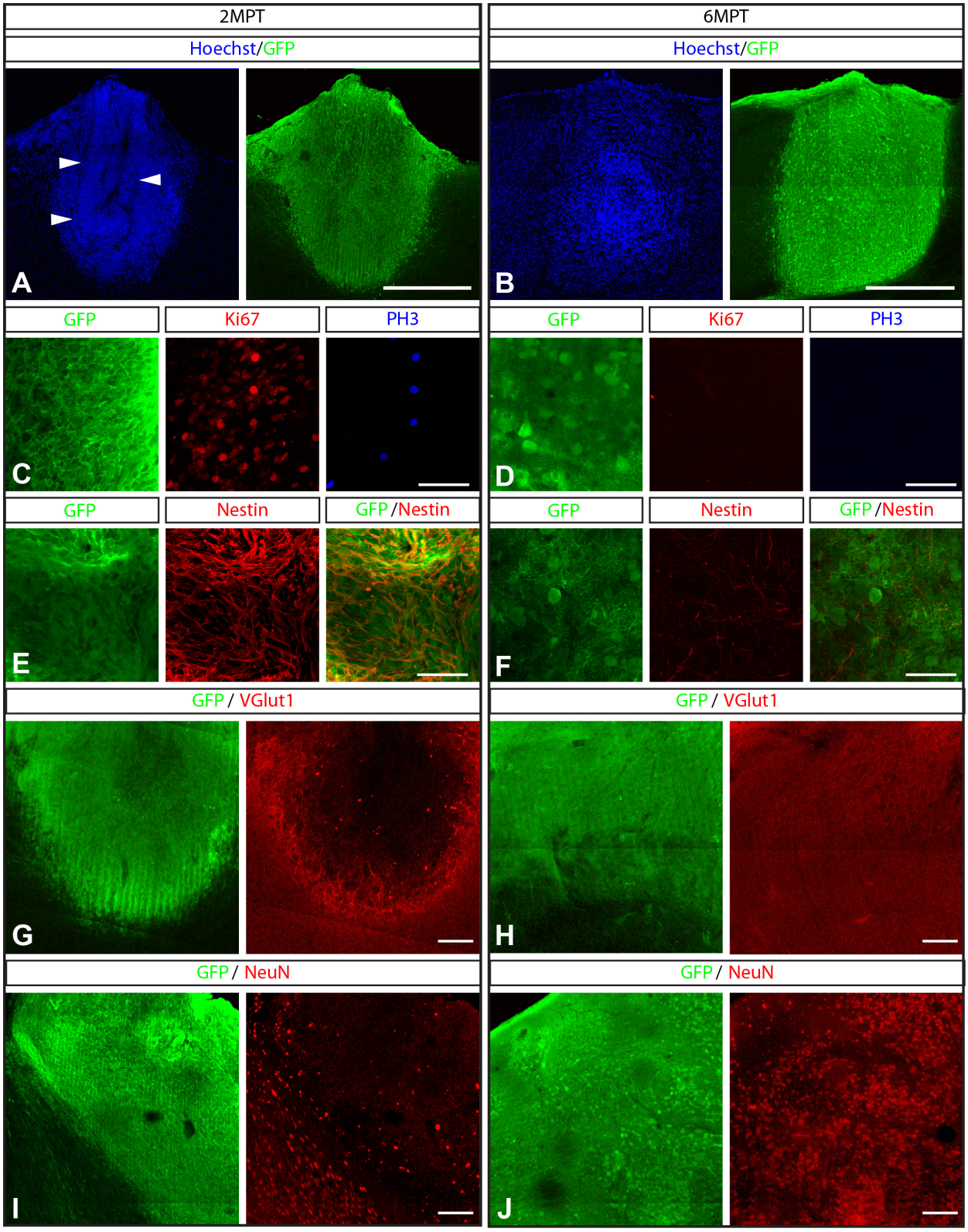

Figure S1. Gradual maturation of human transplants between 2MPT and 6MPT. Related to Figure 1 and Figure 2

(A-B) Representative immunofluorescence images of grafts at 2MPT (A) and 6MPT (B) showing the nuclear staining Hoechst (in blue) and the GFP+ graft (in green). Arrowheads show the presence of rosette-like structures at 2MPT. (C-F) Immunofluorescence images showing the GFP+ graft (in green) and the proliferative/progenitor markers Ki67 (in red; C-D), PH3 (in blue; C-D), and Nestin (in red; E-F) at 2MPT (C,E) and 6MPT (E,F). (G-J) Immunofluorescence images showing the GFP+ graft (in green) and the mature neuronal markers VGlut1 (in red; G-H), and NeuN (in red; I-J) at 2MPT (G,I) and 6MPT (H,J). (A-B) Composite picture views made from the stacked confocal images showing the whole transplant after 2MPT (A) and 6MPT (B). Scale bars 500 µm (A-B); 50 µm (C-F); 100 µm (G-J).

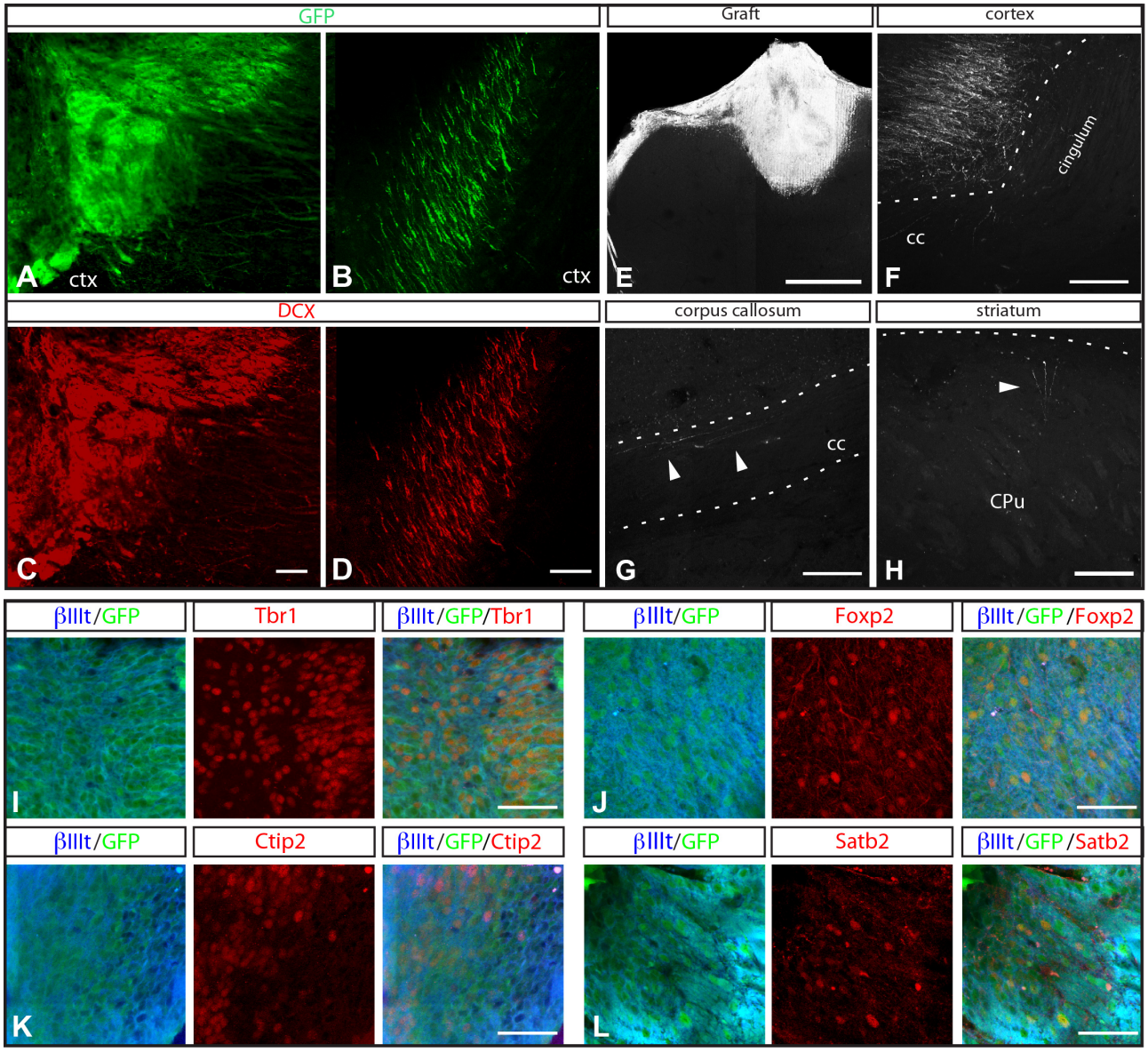

Figure S2. Transplanted human ESC-derived neurons display short-range axonal projections and immature growth cones at 2MPT. Related to Figure 1 and Figure 2

(A-D) Immunofluorescence images showing GFP+ somas and GFP+ neural processes (in green; A-B), and the immature neuronal growth cone marker DCX (in red; C-D) in grafted hESC-derived neurons in the cortex 2MPT. (E-H) Immunofluorescence images showing the location of the GFP+ graft (E), neighbouring GFP+ ipsilateral cortical projections (F), and a few fibers along the corpus callosum (G) and in the striatum (H). Arrowheads show the few fibers detected. Ctx, cortex; cc, corpus callosum; CPu, caudate putamen. (I-L) Immunofluorescence images showing the GFP+ graft (in green), beta III tubulin (in blue) and the deep layer cortical neuronal markers Tbr1 (in red; I); Foxp2 (in red; J); Ctip2 (in red; K) and the upper layer cortical neuronal marker Satb2 (in red; L) 2 MPT. (E) Composite picture view made from the stacked confocal images showing the transplant and few fibers 2MPT. cc, corpus callosum; CPu, caudate putamen (striatum). Scale bars 50 μm (A-D; I-L); 500 μm (E); 100 μm (F-H).

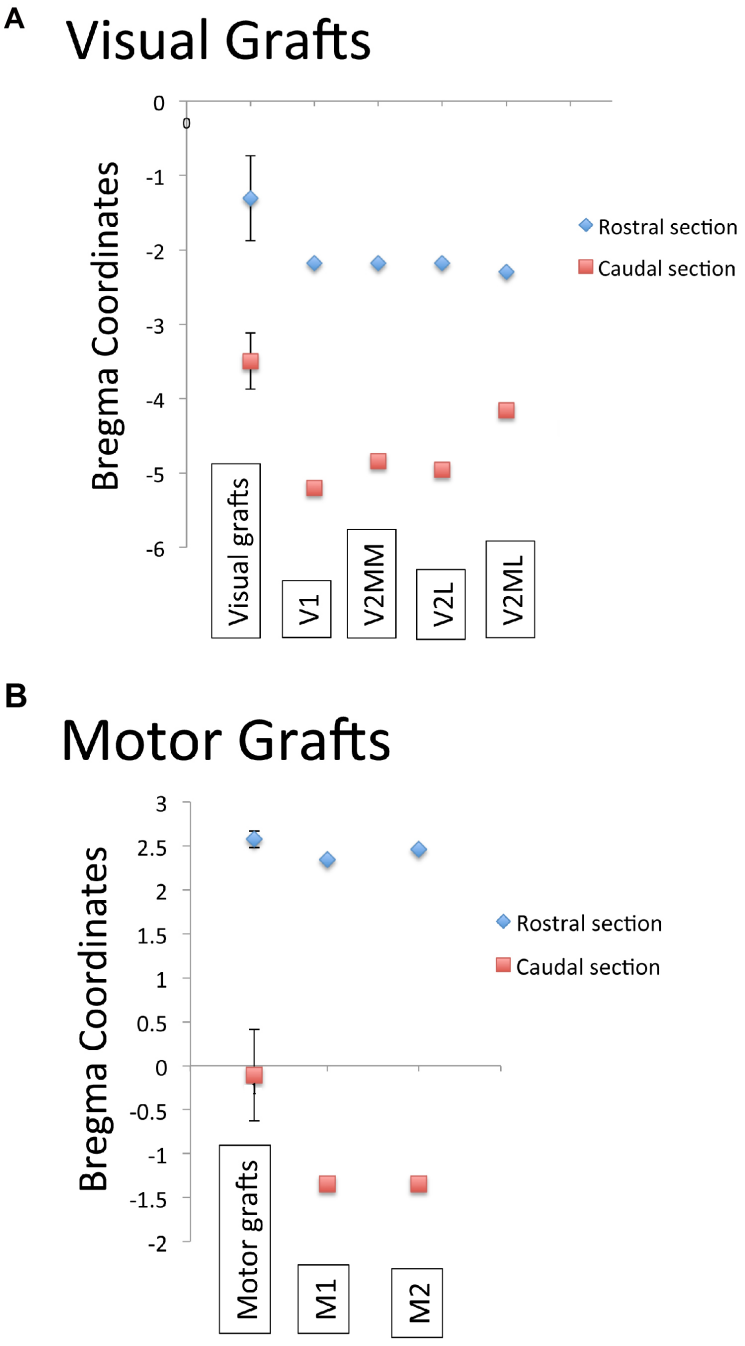

Figure S3. Transplants into Motor and Visual cortex localize within motor and visual cortical areas, respectively. Related to Figure 4 and Figure 5.

(A,B) Quantification of the graft bregma coordinates following transplantation into the visual (A) or motor cortex (B) in comparison with the location of visual and motor host cortical areas. Data are presented as mean bregma coordinates ± s.e.m., (n=7 visual grafts; n=4 motor grafts) of the most rostral section (blue diamond symbol) and the most caudal section (red square symbol) of the grafts. The most rostral and the most caudal bregma coordinates of host visual and motor cortical areas are also represented (A-B). V1, primary visual cortex; V2MM, secondary visual cortex, mediomedial area; V2L, secondary visual cortex, lateral area; V2ML, secondary visual cortex, mediolateral area; M1, primary motor cortex; M2, secondary motor cortex.

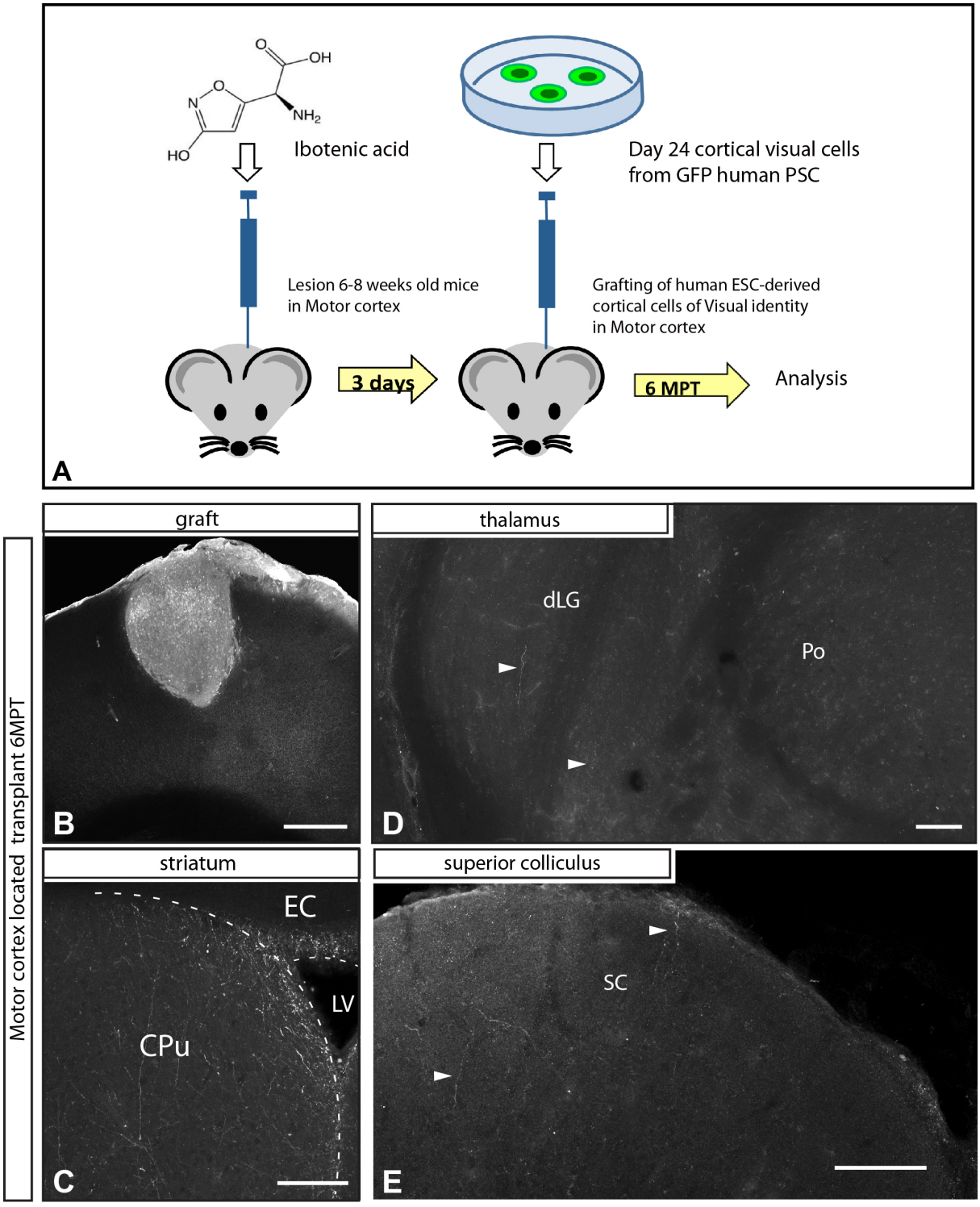

Figure S4. Transplants into the Motor cortex of human ESC-derived cortical neurons show few long-range projections at 6MPT. Related to Figure 4 and Figure 5.

(A) Experimental scheme of the lesioning/transplantation experiments in motor cortex. (B) GFP+ graft location is detected by immunofluorescence in the motor cortex at 6MPT. (C-E) Following motor cortex transplantation GFP+ axonal projections are detected by immunofluorescence in different regions of the mouse brain 6MPT. Fibers are detected in the striatum (CPu) (C), however, almost no fibers are detected in thalamic (dLG) (D), or midbrain structures (SC) (E). dLG, dorsal lateral geniculate; Po, posterior nucleus; EC, external capsule; LV, lateral ventricule; CPu, caudate putamen; SC, superior colliculus. (B,D-E) Composite picture views made from the stacked confocal images showing the whole transplant located into the motor cortex (B), dLG and Po, thalamus (D), and the superior colliculus, midbrain (E) at 6MPT. dLG, dorsolateral geniculate nucleus; Po, posterior thalamic nuclear group; CPu, caudate putamen; ec, external capsule; LV, lateral ventricle; SC, superior colliculus. Scale bars 500 µm (B), 100 µm (B-D).

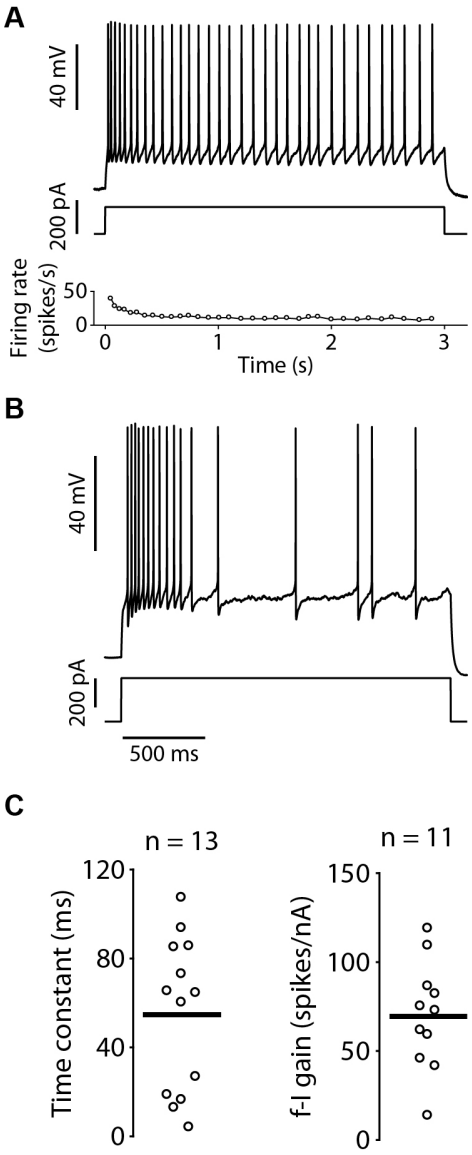

Figure S5. Transplanted human ESC-derived neurons into the visual cortex show mature electrophysiological properties at 8-9 MPT. Related to Figure 6.

(A) Sample membrane voltage traces of a cell showing a high accommodation index (only in 3 out of 11 cells in which APs were recorded), evoked by the intracellular injection of hyperpolarizing and depolarizing current steps. (B) Sample membrane voltage traces of a cell showing a typical interneuron-like discharge profile (only in 1 out of 11 cells recorded), evoked by the intracellular injection of hyperpolarizing and depolarizing current steps. (C) Single-cell passive (left) and active (right) membrane properties: open circles correspond to individual cells, with the bar representing the population mean. Both passive and active properties are in the ranges typically observed in cortical pyramidal neurons.

Supplemental Experimental Procedures

Human pluripotent stem cell culture

Experiments were performed using the H9 ESC line (Wicell) stably expressing GFP under the control of chicken β-actin promoter (H9-GFP line) generated previously (Espuny-Camacho et al., 2013). Human ESC were cultured and routinely passaged on mitotically inactivated mouse embryonic fibroblasts (MEFs), and routinely assayed for the expression of pluripotentcy markers, as previously described (Thomson, 1998).

Human ESC differentiation into cortical progenitors and neural cells.

Human ESC were differentiated towards cortical progenitors and neurons as previously described (Espuny-Camacho et al., 2013). In brief, human pluripotent stem cells were dissociated using Stem-Pro Accutase on day -2, (Invitrogen A11105) and plated on matrigel (BD, hES qualified matrigel) coated-coverslips/dishes at low confluency (5,000–10,000 cells/cm2) in MEF-conditioned hES/hiPS medium supplemented with ROCK inhibitor for cell survival (Y-27632; 10 μM Calbiochem, 688000). On day 0 of the differentiation, the medium was changed to "default differentiation medium" DDM supplemented with B27 (10 ml B27 per 500 ml DDM, GIBCO) for better human progenitor survival and with Noggin for neuroectoderm acquisition (100 ng/ml, R&D Systems). The medium was replenished every 2 days. After 16 DIV, noggin was withdrawn, and the medium was changed to DDM, supplemented with B27 (GIBCO), and changed every 2 days. At 24 DIV the human cortical progenitors were manually dissociated using a Pasteur cut pipette and a dilution of 100,000 cells per microliter was prepared for the animal transplantation experiments, as described in (Espuny-Camacho et al., 2013).

Animal lesioning and grafting.

All mouse experiments were performed with the approval of the Université Libre de Bruxelles Committee for animal welfare. Six- to 8-week-old adult NOD/SCID mice were anesthetized with ketamine and xylazine, followed by focal stereotactic injections of ibotenic acid to obtain focal cortical lesions performed either at the visual or motor cortex, as described before (Michelsen et al., 2015). In brief, the mice were placed in a stereotaxic frame, the dorsal surface of the head was shaved and a hole was drilled in the skull above the visual or motor cortex. 20 mg of ibotenic acid in 1μl distilled water was injected using a Hamilton syringe in the left visual (coordinates in mm B -3,1 / L - 2,4 / D 0,7) or left motor cortex (coordinates in mm B +1,2 / L 1,5 / D 0,8). The wound was closed and the mice left to recover in individual cages. Three days later, around 100.000 human ESC-derived cortical progenitors (in 0.5-1μl) were injected in the same coordinates, following the same procedure. The mice were again placed in individual cages for full recovery after surgery. A total number of 58 cases were analysed (n=37 for motor located transplants and n=21 for visual located transplants).

Tissue preparation and immunofluorescence.

For microscopy analysis, the mice were anesthetized with ketamine/xylazine and perfused with phosphate-buffered saline followed by 4% paraformaldehyde. The brain was removed and postfixed in the same fixative overnight and then cut in 75 μm slices on a Leica vibroslicer.

Immunofluorescence on grafted brains was performed as described previously (Espuny-Camacho et al., 2013). Briefly, sections were permeabilised and blocked for one hour at room temperature in solution containing 3% goat serum, 0.3% Triton X-100. The sections were then incubated overnight at 4 degrees with primary antibodies diluted in the same solution (for list of primary antibodies see table below). The following day PBS was used to wash the primary antibodies and the sections were incubated in the solution with secondary antibodies containing 3% goat serum, 0.3% Triton X-100 for 1 h at room temperature (for list of secondary antibodies see table below).

Antigen retrieval, when necessary, was performed by microwave boiling the slides in 10 mM tri-Sodium Citrate buffer pH 6.0 (VWR). Nuclei staining was performed using a specific anti-human nuclei antibody (see table below) or the pan-nuclear staining Hoechst.

Immunofluorescence images were acquired using a Zeiss LSM 510 META confocal microscope driven by ZEN 2009 software and 20x, 40x, 60x objectives and green, red, far-red and 2P lasers. Images were acquired as Z-series of stacks, 16-bit, 1024x1024 arrays that were consequently converted to maximum intensity projections (ImageJ). Image processing was performed with ImageJ and Adobe Photoshop/Illustrator (Adobe Systems) for preparation of multipanel Figures. Composite picture views were stitched manually from the individual confocal Z-series of stack images using Fiji and Adobe Photoshop.

Primary antibodies	Species	Company	Catalog Number	Dilution

beta III tubulin (Tuj1)	mouse	Covance	MMS-435P	1/1000
beta III tubulin	rabbit	Covance	PRB-435P	1/1000
beta III tubulin	chicken	Chemicon	AB9354	1/1000
Brn2	rabbit	Santa Cruz Biotech	Sc-6029	1/300
Couptf1	mouse	Abcam	Ab41858	1/500
CTIP2	rat	Abcam	ab18465-100	1/500
Doublecortin	rabbit	Cell Signaling		1/500
Foxg1	rabbit	Abcam	ab18259	1/100
Foxp2	rabbit	Abcam	ab16046-100	1/5.000
GFP	rabbit	Invitrogen	A6455	1/2000
GFP	chicken	Abcam	AB13970-100	1/2000
Homer1	rabbit	Synaptic Systems	160 003	1/1.000
Human Nu antigen, clone 235-1	mouse	Chemicon	MAB1281	1/500
Human NCAM	mouse	Santa Cruz	ERIC 1 sc-106	1/500
Ki67	rabbit	Abcam	833-500	
MAP2	mouse	Sigma	M1406-2ml	1/2000
Nestin	mouse	Covance	MMS-570P	1/1000
NeuN	mouse	Millipore	MAB377	1/300
Pax6	rabbit	Covance	PRB-278P	1/2.500
PH3	rat			1/1000
Satb2	rabbit	Abcam	ab34735	1/1000
Synaptophysin	mouse	Synaptic Systems	101 011	1/1.000
Tau	rabbit	DAKO	0024	1/500
Tbr1	rabbit	Gift from Hevner		1/10.000
VGlut1	rabbit	Synaptic Systems	135 302	1/1000

Secondary antibodies	**Species**	**Company**	**Dilution**
anti-mouse Alexa Fluor 488	donkey	Invitrogen	1/500
anti-rabbit Alexa Fluor 488	donkey	Invitrogen	1/500
anti-chicken Alexa Fluor 488	chicken	Invitrogen	1/500
anti-mouse cyanin3	donkey	Jackson Immunoresearch	1/500
anti-rabbit cyanin3	donkey	Jackson Immunoresearch	1/500
anti-rat cyanin3	donkey	Jackson Immunoresearch	1/500
anti-goat cyanin3	donkey	Jackson Immunoresearch	1/500
anti-mouse cyanin5	donkey	Jackson Immunoresearch	1/500
anti-rabbit cyanin5	donkey	Jackson Immunoresearch	1/500

Quantification of axonal projections following grafting.

Total number of GFP positive fibers and percentage of GFP positive fibers present at different cortical targets: striatum, thalamus and midbrain, were manually counted on coronal brain sections. GFP positive fibers were detected following immunofluorescence staining using GFP antibody, and were visualized using a Zeiss Axioplan upright fluorescence microscope equipped with 20x and 40x dry objectives.

For the striatum, the total number of fibers was counted in 1/6 of the sections collected for each individual brain. For the thalamus and midbrain, fibers were counted in 1/2 of the sections collected for each individual brain. Data are represented as mean ± s.e.m.. For the percentage of fibers, a total number of 10 and 8 animals were used for

quantification following transplantation into the visual and motor cortex, respectively. Statistical analyses were performed using the non-parametric Wilcoxon signed-rank test for paired data (to compare results in different brain areas in the same group of mice, either in visual or motor grafted mice), *p < 0.05, **p < 0.01. For the total number of fibers, 11 and 17 animals were used for quantification following transplantation into the visual and motor cortex, respectively. Statistical analyses were performed using the non-parametric Mann-Whitney test for unpaired data (to compare results in different groups of mice: visual versus motor grafted mice), *p < 0.05, **p < 0.01; ***p<0.001.

Quantification of the graft bregma coordinates following transplantation into the visual and motor cortex.
The bregma coordinates for the location of grafts following transplantation into the visual or motor cortex was analysed in coronal sections corresponding to 1/6 of the collected brain sections. Grafts were visualised by immunostaining using GFP antibody. The most rostral and the most caudal brain section containing the graft was analysed for bregma coordinates using the mouse brain atlas as a reference (Franklin and Paxinos, third edition 2007). Data are presented as mean bregma coordinates ± s.e.m., (n=7 visual grafts; n=4 motor grafts).

Quantification of the percentage of Tbr1+ and Foxp2+ cells in motor and visual located transplants.
The percentage of Tbr1 and Foxp2 positive cells detected among the total number of GFP and Hu Nuclei positive cells (human grafted cells) was determined on confocal acquired images using Fiji/ImageJ software from immunofluorescence stained brain sections. Confocal images were acquired using a Zeiss LSM 510 META microscope driven by ZEN 2009 software and 20x objective and green, red, far-red and 2P lasers. Images were acquired as Z-series of stacks of 5 μm step, 16-bit, 1024x1024 arrays that were consequently converted to maximum intensity projections and threshold adjusted using Default method to isolate specific Tbr1 and Foxp2 fluorescence (ImageJ). The percentage of Tbr1+ and Foxp2+ cells (number of cells over the total GFP+ HuNuclei+ counted) was quantified in 3 images blindly acquired from 2-3 different sections per animal. Data are represented as mean percentage ± s.e.m. (Tbr1 n=4 animals; 1.800-2.856 neurons; Foxp2 n=3-4 animals; 1.113-2.587 neurons). Statistical analysis was performed following Student's t test: n.s= non-significant.

Quantification of the percentage of Couptf1+ cells in motor and visual located transplants.
The percentage of Couptf1 positive cells detected among the total number of GFP positive cells (human grafted cells) was manually determined on confocal acquired images using Fiji/ImageJ software from immunofluorescence stained brain sections. Confocal images were acquired using a Zeiss LSM 510 META microscope driven by ZEN 2009 software and 40x objective and green, red, far-red and 2P lasers, using identical acquisition parameters as 16-bit, 1024x1024 arrays. Z-series stacks were then converted in ImageJ to maximum intensity projections and threshold adjusted using Triangle method to isolate specific Couptf1 fluorescence. The percentage of Couptf1+ cells (number of cells over the total GFP+ counted) was quantified in 4 different areas blindly set in all images. Data are represented as mean percentage ± s.e.m. (n=3 animals; 1.400-2.116 neurons). Statistical analysis was performed following Student's t test: *p < 0.05.

Quantification of the graft volume in motor and visual located transplants
The graft volume was measured from confocal acquired images from the graft in serial coronal sections corresponding to a sixth of the mouse brain. Mouse brain sections were immunostained with GFP antibody and confocal images were acquired using a Zeiss LSM 510 META microscope driven by ZEN 2009 software with a 10x objective using identical acquisition parameters as 16-bit. Z-series stacks of 10 μm step were acquired for a total of 6 steps (60 μm thickness). The volume of the graft contained within one individual section was calculated using Fiji/plugin software, and the total graft volume corresponding to 1/6 of the brain was determined by adding the individual volumes of each of the sections with a graft. Data are represented as mean percentage ± s.e.m. (n=8 animals grafted into the visual cortex; n=8 animals grafted into the motor cortex). Statistical analysis was performed following Student's t test: n.s= non-significant.

Quantification of the proportion of transplants with subcortical projections
We quantified the proportion of visual and motor located transplants projecting GFP positive fibers into the striatum, thalamus and midbrain over the total number of visual and motor transplanted animals. Quantification was performed by manual counting of the axonal projections in immunofluorescence stained brain sections using the GFP antibody. Images were acquired using a Zeiss Axioplan upright confocal microscope equipped with 20x and 40x dry objectives.
For the quantification of the proportion of animals with fibers present in the striatum, we quantified 1/6 of the sections collected for each individual brain. For the quantification of the proportion of animals with fibers in thalamus and midbrain, 1/2 of the sections collected for each individual brain were analysed. Data are represented as mean percentage ± s.e.p. (visual grafts: n=11 animals; motor grafts: n=17 animals). Statistical analysis was performed following Z test for proportions: ns= non-significant; *p < 0.05.

***Ex vivo* electrophysiology**
Electrophysiological recordings were performed on grafted neurons in acute brain slices from mice at 8 and 9 months post-transplantation. Acute brain slices were obtained as follows: Mice were deeply anesthetized with a mixture of

ketamine and xylazine, and transcardially perfused with ice-cold solution containing (in mM) 80 NaCl, 2.5 KCl, 1.25 NaH_2PO_4, 1 $CaCl_2$, 5 $MgCl_2$, 30 $NaHCO_3$, 25 D-glucose and 75 sucrose (gassed with 95% O_2/5% CO_2). The brain was rapidly removed, trimmed by cutting off cerebellum and hindbrain directly behind the occipital cortex, and glued to the stage of a VT1000-S vibratome (Leica Instruments, Nussloch, Germany) to cut 300 m thick coronal slices in the same solution at 4 °C. Slices were incubated after cutting in artificial CSF (aCSF) containing (in mM) 125 NaCl, 2.5 KCl, 1.25 NaH_2PO_4, 2 $CaCl_2$, 1 $MgCl_2$, 30 $NaHCO_3$ and 25 D-glucose (gassed with 95% O_2/5% CO_2) for at least 20 minutes and stored thereafter at room temperature for up to 7 h. For recording one slice at a time was transferred to a chamber and continuously perfused with aCSF at 1.5 ml/min. Transplanted cells were identified by their EGFP fluorescence and visualized using an upright microscope equipped with infrared differential interference contrast (Leica Microsystems, DMLFS, Belgium). Recordings were performed at 33 ± 1 °C. For recordings, patch pipettes (resistance 6–9 M containing (in mM): 115 K-gluconate, 20 KCl, 10 HEPES, 4 Mg-ATP, 0.3 Na_2-GTP, 10 Na_2-phosphocreatine, pH adjusted to 7.3 with KOH. Current clamp recordings were performed with an EPC 10 patch clamp amplifier (HEKA Electronics, Lambrecht/Pfalz, Germany): neither bridge balance nor capacitance compensation were used online: rather, electrode kernels were estimated throughout the experiment by following the procedure described in (Brette et al., 2008) and subsequently used to compensate offline the recorded data. Liquid junction potentials were left uncorrected. Signals were recorded at a rate of 20 kHz. All electrophysiological recordings were analyzed using MATLAB (The Mathworks, Natick, MA). To deliver bipolar extracellular electrical stimuli and elicit compound synaptic responses, we used an ISO-Flex stimulus isolator (AMPI, Israel) connected to two platinum wires inserted in a theta-glass pipette (1401021, Hilgenberg, Malsfeld, Germany) filled with aCSF. This electrode was placed at distances between 100 and 400 μm from the recorded neuron and current-controlled stimuli had amplitude in the range 100-1000 μA and duration of 100 μs. In some experiments, synaptic inputs were blocked by adding to the bath selective antagonists of ligand-gated channels (i.e., AP-V, 50 μM; CNQX, 20 μM; GABAzine, 10 μM). All the chemicals were from Sigma, Belgium.

Accommodation index

In order to quantify the degree of spike frequency adaptation, the accommodation index A was computed according to (Druckmann et al., 2007) as

$$A = \left(N_{spks} - 4 - 1\right)^{-1} \cdot \sum_{q=4}^{N_{spks}-1} \left(\mathrm{ISI}_q - \mathrm{ISI}_{q-1}\right) / \left(\mathrm{ISI}_q + \mathrm{ISI}_{q-1}\right) \tag{6}$$

where N_{spks} is the number of spikes evoked by a constant depolarizing step of current, ISI_q is the q-th inter-spike interval, and where the first four spikes were always discarded from the analysis, to ensure that the firing discharge had reached a steady-state regime.

Supplemental References

Brette, R., Piwkowska, Z., Monier, C., Rudolph-Lilith, M., Fournier, J., Levy, M., . . . Destexhe, A. (2008). High-resolution intracellular recordings using a real-time computational model of the electrode. *Neuron, 59*(3), 379-391. doi:10.1016/j.neuron.2008.06.021

Druckmann, S., Banitt, Y., Gidon, A., Schürmann, F., Markram, H., and Segev, I. (2007). A novel multiple objective optimization framework for constraining conductance-based neuron models by experimental data. Front. Neurosci. *1*, 7–18.

Franklin, K.B.J. and Paxinos, G., (Third edition 2007). The mouse brain in stereotaxic coordinates. Academic Press.

Thomson, J.A. (1998). Embryonic Stem Cell Lines Derived from Human Blastocysts. Science (80-.). *282*, 1145–1147.